Crystal Structure, Conformational Analysis, and Molecular Dynamics of Tetra-*O*-Methyl-(+)-Catechin

FRANK R. FRONCZEK,[1] RICHARD W. HEMINGWAY,[2] G. WAYNE MCGRAW,[2,3] JAN P. STEYNBERG,[2,4] CARIN A. HELFER,[5] and WAYNE L. MATTICE[5]

[1]Department of Chemistry, Louisiana State University, Baton Rouge, Louisiana 70803-1804, USA; [2]Southern Forest Experiment Station, 2500 Shreveport Highway, Pineville, Louisiana 71360-5500, USA; [3]Department of Chemistry, Louisiana College, Pineville, Louisiana 71360, USA; [4]Department of Chemistry, University of the Orange Free State, Bloemfontein, South Africa; and [5]Department of Polymer Science, The University of Akron, Akron, Ohio 44325-3909, USA

SYNOPSIS

The structure of tetra-*O*-methyl-(+)-catechin has been determined in the crystalline state. Two independent molecules, denoted structure A and structure B, exist in the unit cell. Crystals are triclinic, space group P1, $a = 4.8125(2)$ Å, $b = 12.9148(8)$ Å, $c = 13.8862(11)$ Å, $\alpha = 86.962(6)°$, $\beta = 89.120(5)°$, $\gamma = 88.044(5)°$, $Z = 2$, $D_c = 1.336$ g cm^{-3}, $R = 0.033$ for 6830 observations. The heterocyclic rings of the crystal structures are compared to previous results for 8-bromotetra-*O*-methyl-(+)-catechin, penta-*O*-acetyl-(+)-catechin, and (−)-epicatechin. One of the two molecules has a heterocyclic ring conformation similar to that observed previously for (−)-epicatechin, and the other has a heterocyclic ring conformation similar to one predicted earlier in a theoretical analysis of dimers of (+)-catechin and (−)-epicatechin. Both structure A and structure B in the crystal have heterocyclic ring conformations that place the dimethoxyphenyl substituent at C(2) in the equatorial position. However, this heterocyclic ring conformation does not explain the proton nmr coupling constant measured in solution. Molecular dynamics simulations show an equatorial ⇌ axial interconversion of the heterocyclic ring, which can explain the nmr results.

INTRODUCTION

Proanthocyanidins are the second most abundant class of polyphenols (after lignin) in the plant kingdom.[1,2] Because their biological and commercial significance generally rests on the complexation of these phenolic polymers with other biopolymers such as proteins and carbohydrates, it is essential that more is learned about the conformational properties of these compounds. The most widely distributed group of proanthocyanidins in plants is the 3,5,7,3′,4′-pentahydroxyflavans (procyanidins) that are usually made up of two monomer units (+)-catechin and (−)-epicatechin. These two compounds differ from one another only in the stereochemistry of the attachment of the hydroxy group at C(3), as depicted in Figure 1. Oligomers and polymers are formed by interflavan bonds from C(4) to C(8), or from C(4) to C(6), in successive monomer units. Steric interactions impose severe restrictions to internal rotation about the interflavan bond in either case.[3-5] The conformational energy vs dihedral angle at the interflavan bond exhibits two minima separated by rotations of about 180°. The difference in energy of these two minima depends on whether the interflavan bond is from C(4) to C(6) or from C(4) to C(8), on the stereochemistry of its attachment at C(4), and the identity of the monomers.[3-7] If the difference in energy is sufficiently large so that one conformation completely dominates the other, the oligomer will form a helix.[1,7-9]

The conformations of the individual monomer units have a strong influence on the steric interactions that control the manner in which the confor-

Biopolymers, Vol. 33, 275–282 (1993)
 CCC 0006-3525/93/020275-08

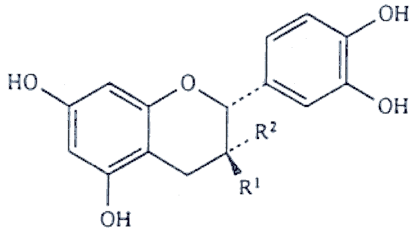

(+) - catechin $R^1 = OH, R^2 = H$
(-) - epicatechin $R^1 = H, R^2 = OH$

Figure 1. Covalent structure of (+)-catechin and (−)-epicatechin.

mational energy depends on the dihedral angle at the interflavan bond. Consequently, it is important to develop a complete understanding of the conformations of the monomers, and the manner in which these conformations are altered by changes in their covalent structures as a consequence of the introduction of substituents. Crystal structures of monomers and their derivatives provide an important data base for testing the accuracy of the algorithms used for the theoretical study of the conformations of the polymeric procyanidins. The crystal structure of (−)-epicatechin is available at high resolution,[10] but (+)-catechin has resisted crystallization in a form amenable to a structure determination. The absence of a crystal structure of (+)-catechin produces special interest in the structures of its derivatives, several of which are available.[11-15] One of these structures, for penta-*O*-acetyl-(+)-catechin, is different from the other structures in two important aspects. It is the only structure in which the heterocyclic ring adopts a conformation that places the disubstituted phenyl group at C(2) in an axial position, and it is the only crystal structure that exhibits conformational disorder.[14] The disorder arises from the partial occupancy of two different positions by the acetoxy group at C(3).

The derivative of interest in the present article, tetra-*O*-methyl-(+)-catechin, occupies two different ordered structures in the unit cell. We shall describe these two structures, compare them with previously reported structures for (−)-epicatechin and derivatives of (+)-catechin, present a conformational analysis that is of assistance in the interpretation of the occupancy of two structures in the unit cell, and show that the two structures interconvert very rapidly in the isolated molecule. In addition, we shall discuss the conformation of tetra-*O*-methyl-(+)-catechin in solution as determined from experimental proton nmr coupling constants combined with molecular dynamics simulations.

MATERIALS AND METHODS

Tetra-*O*-Methyl-(+)-Catechin

The compound was made from (+)-catechin by methylation with diazomethane followed by Si-gel column chromatography eluting with diethylether–methanol. The compound was crystallized from diethylether–methanol by slow evaporation of solvent in a fume cupboard to give light-tan colored needles: mp 143–144°, $[\alpha]_D$ − 11.0°, lit.[16] mp 143–144°C, $[\alpha]_D$ − 13.6°; found C = 65.7, H = 6.47; calc. C = 65.9, H = 6.36%. ^{1}H-nmr ($CDCl_3$) δ: 2.55 (dd; 9.0, 16.0 Hz, H-4ax); 3.05 (dd; 5.5, 16.0 Hz, H-4eg). 3.72, 3.76, 3.85 (3H, 3H, 6H, Ar-O-CH_3, 3.95 (br-m, H-3); 4.63 (d, 8.1 Hz, H-2), 6.07 (2H, H-6 and H-8); 6.84, 8.92, 7.21 (3H, H-5′, H-6′, H-2′).

Data Collection and Structure Solution (X-Ray)

A colorless crystal of dimensions 0.12 × 0.25 × 0.50 mm was used for data collection on an Enraf-Nonius CAD4 diffractometer equipped with Cu-K_α radiation (λ = 154.184 pm) and a graphite monochromator. Crystal data are $C_{19}H_{22}O_6$, M = 46.4, triclinic space group P1, Z = 2, a = 4.8125(2) Å, b = 12.9148(8) Å, c = 13.8862(11) Å, α = 86.962(6)°, β = 89.120(5)°, γ = 88.044(5)°, V = 861.2(1) Å^3, D_C = 1.336 g cm^{-3}, μ(CuK$_\alpha$) = 7.8 cm^{-1} at 296 K. A full sphere of data having $2 < \theta < 75°$ was collected by $\omega - 2\theta$ scans of variable rate, and one hemisphere was recollected. Data reduction included corrections for background, Lorentz polarization, and absorption. The latter corrections were based on ψ scans, with minimum relative transmission coefficient 85.27%. Redundant data were averaged (R_{int} = 0.007), yielding 6921 unique data, of which 6830 had $I > 3\sigma(I)$ and were used in the refinement. The structure was solved using SHELXS[17] and refined by full-matrix least squares based on F with weights $w = \sigma^{-2}(F_0)$. C and O atoms were refined anisotropically; H atoms were located by ΔF, and included as fixed contributions except for OH hydrogen atoms, which were refined isotropically. A secondary extinction coefficient refined to a value of g = 1.18(4) × 10^{-5}. The final value of R_w was 0.04873, while the mirror-image structure refined to R_w = 0.04924. The better fit for the R isomer at C2 agrees with the absolute configuration determined for 8-bromotetra-*O*-methyl-(+)-catechin.[11] Maxi-

mum and minimum residual electron densities are 0.35 and -0.28 eÅ^{-3}.

Conformational Energy Analysis

Starting with the two structures of tetra-*O*-methyl-(+)-catechin in the crystalline state, optimized geometries were obtained by minimization of the energy functions. The conjugate gradient method was used for minimization. Electrostatic interactions were ignored because they have been shown previously to be of little consequence for the conformations of this class of molecules.[10] Termination of the minimization procedure occurred when the energy change was less than 0.1 cal mol^{-1}.

Molecular Dynamics Simulations

Two molecular dynamics simulations were run in vacuo for 4.5 ns with a time step of 0.25 fs using Sybyl 4.1c (Tripos Associates, Inc., St. Louis, Missouri). In one trajectory, the initial coordinate set was taken to be the coordinates of crystal structure A, which has the heterocyclic ring in the equatorial conformation. In the second trajectory, the dihedral angle for rotation about the C(2) — C(3) bond was initially set at 300°, causing the heterocyclic ring to be in the axial conformation. Each of these initial structures was minimized using the conjugate gradient method for 50 steps. The Verlet algorithm was then used to integrate the equations of motion in the dynamics simulation. First the molecules were heated from 0 to 300 K over 700 fs with the starting velocities generated from a Boltzmann distribution. The system was then equilibrated for 50 ps before computing the trajectory for 4.5 ns. The trajectories were run at constant temperature with the velocities rescaled. The coordinates were recorded at intervals of 500 fs for subsequent analysis.

RESULTS AND DISCUSSION

Structure in the Crystalline State

The unit cell of tetra-*O*-methyl-(+)-catechin has two independent molecules, which will be denoted as crystal structure A and crystal structure B. The two crystal structures are depicted in Figure 2. The coordinates for the C, O, and hydroxy H atoms in each of these crystal structures are listed in Table I. Differences between the two crystal structures are the dihedral angles for rotation around the C(3) — O(2) bond and the O(6) — C(20) bond. The dihedral angles for the C(3) — O(2) bond are

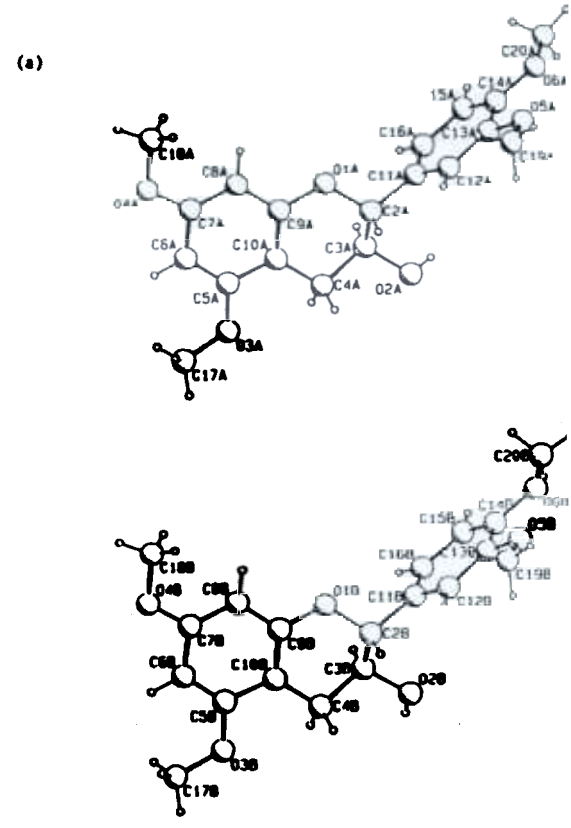

Figure 2. (a) Structure A and (b) structure B of tetra *O*-methyl-(+)-catechin in the crystalline state.

−82.8° and −179.7°, for crystal structure A and crystal structure B, respectively. The O(6) — C(20) bond has dihedral angles of 47.4° and 65.2° for A and B, respectively. There are also subtle differences in the conformations of the heterocyclic rings.

It is clear that the existence of two independent molecules in the unit cell, having different orientations of the hydroxy group, results from optimization of intermolecular hydrogen bonding. Hydroxy group O(2A) donates a hydrogen bond, with an O···O length of 2.994(2) Å, to methoxy oxygen O(4B) in the molecule at $x - 1, y, z + 1$. The angle at hydrogen is 145(2)°. Similarly, hydroxy group O(2B) denotes a hydrogen bond of length 2.968(2) Å to methoxy oxygen O(6A) at $x, y - 1, z - 1$, with angle at H 141(2)°. Thus each molecule is involved in two hydrogen bonds, and these interactions form chains of alternating molecular types along the direction of the *b* axis. This pattern is illustrated in Figure 3.

The fused ring systems of each of the crystal structures of tetra-*O*-methyl-(+)-catechin are depicted in Figure 4. The carbon atoms in the aromatic rings are within 1.3 pm of the mean plane. In the

Table I Coordinates and Thermal Parameters for C, O, and Hydroxy H Atoms in Tetra-*O*-Methyl-(+)-Catechin

Atom	x	y	z	B_{eq} (Å^2)
O1A	1		1	3.52 (2)
O2A	0.5360 (2)	0.80602 (8)	1.11361 (7)	4.00 (2)
O3A	0.7630 (3)	0.76934 (8)	0.76211 (7)	4.59 (2)
O4A	1.3910 (3)	1.0374 (1)	0.68235 (8)	4.93 (2)
O5A	0.4798 (2)	1.21065 (8)	1.30359 (8)	4.02 (2)
O6A	0.8517 (2)	1.13579 (9)	1.42076 (7)	4.08 (2)
C2A	0.7622 (3)	0.9643 (1)	1.05620 (9)	2.97 (2)
C3A	0.7557 (3)	0.84613 (9)	1.06437 (9)	3.05 (2)
C4A	0.7017 (3)	0.8171 (1)	0.95240 (9)	3.20 (2)
C5A	0.9127 (3)	0.8522 (1)	0.78542 (9)	3.43 (2)
C6A	1.0852 (3)	0.9057 (1)	0.7212 (1)	3.90 (3)
C7A	1.2276 (3)	0.9898 (1)	0.7520 (1)	3.68 (2)
C8A	1.1971 (3)	1.0207 (1)	0.8453 (1)	3.44 (2)
C9A	1.0211 (3)	0.9645 (1)	0.90851 (9)	3.04 (2)
C10A	0.8800 (3)	0.8792 (1)	0.88159 (9)	2.97 (2)
C11A	0.7900 (3)	1.00598 (9)	1.15464 (9)	2.89 (2)
C12A	0.6153 (3)	1.0886 (1)	1.18168 (9)	2.99 (2)
C13A	0.6398 (3)	1.13030 (9)	1.27043 (9)	2.96 (2)
C14A	0.8419 (3)	1.0892 (1)	1.33484 (8)	2.97 (2)
C15A	1.0159 (3)	1.0082 (1)	1.30787 (9)	3.24 (2)
C16A	0.9900 (3)	0.9667 (1)	1.2181 (1)	3.27 (2)
C17A	0.7559 (7)	0.7461 (1)	0.6640 (1)	7.37 (5)
C18A	1.5393 (4)	1.1249 (1)	0.7067 (1)	5.01 (3)
C19A	0.3105 (3)	1.2684 (1)	1.2359 (1)	4.47 (3)
C20A	1.0542 (4)	1.0962 (1)	1.4885 (1)	4.61 (3)
H2OA	0.583 (4)	0.800 (2)	1.168 (2)	5.4 (5)
O1B	0.9527 (2)	0.53359 (7)	0.54071 (6)	3.30 (2)
O2B	0.5306 (2)	0.30909 (8)	0.50653 (7)	3.89 (2)
O3B	0.8701 (3)	0.50863 (9)	0.20321 (7)	4.68 (2)
O4B	1.4298 (2)	0.76814 (8)	0.32533 (8)	4.30 (2)
O5B	0.3743 (3)	0.4936 (1)	0.89015 (7)	4.64 (2)
O6B	0.7219 (3)	0.3501 (1)	0.95563 (7)	4.55 (2)
C2B	0.7220 (3)	0.46467 (9)	0.55598 (8)	2.75 (2)
C3B	0.7469 (3)	0.37947 (9)	0.48461 (9)	2.88 (2)
C4B	0.7196 (3)	0.4282 (1)	0.38279 (9)	3.11 (2)
C5B	0.9810 (3)	0.5594 (1)	0.27651 (9)	3.38 (2)
C6B	1.1564 (3)	0.6417 (1)	0.2634 (1)	3.80 (3)
C7B	1.2591 (3)	0.6859 (1)	0.3440 (1)	3.35 (2)
C8B	1.1896 (3)	0.6494 (1)	0.43679 (9)	3.05 (2)
C9B	1.0107 (3)	0.56625 (9)	0.44703 (8)	2.79 (2)
C10B	0.9037 (3)	0.51914 (9)	0.36914 (8)	2.88 (2)
C11B	0.7271 (3)	0.42907 (9)	0.66120 (8)	2.80 (2)
C12B	0.5389 (3)	0.4748 (1)	0.72469 (9)	3.04 (2)
C13B	0.5447 (3)	0.4491 (1)	0.82280 (9)	3.24 (2)
C14B	0.7351 (3)	0.3727 (1)	0.85838 (9)	3.38 (2)
C15B	0.9210 (3)	0.3269 (1)	0.7952 (1)	3.69 (2)
C16B	0.9199 (3)	0.3559 (1)	0.6971 (1)	3.42 (2)
C17B	0.9311 (6)	0.5449 (2)	0.1072 (1)	6.65 (5)
C18B	1.5537 (4)	0.8109 (1)	0.4051 (1)	4.58 (3)
C19B	0.2089 (4)	0.5810 (2)	0.8583 (1)	5.17 (3)
C20B	0.9308 (5)	0.2807 (2)	0.9954 (1)	6.44 (4)
H2OB	0.547 (4)	0.263 (2)	0.468 (2)	4.9 (4)

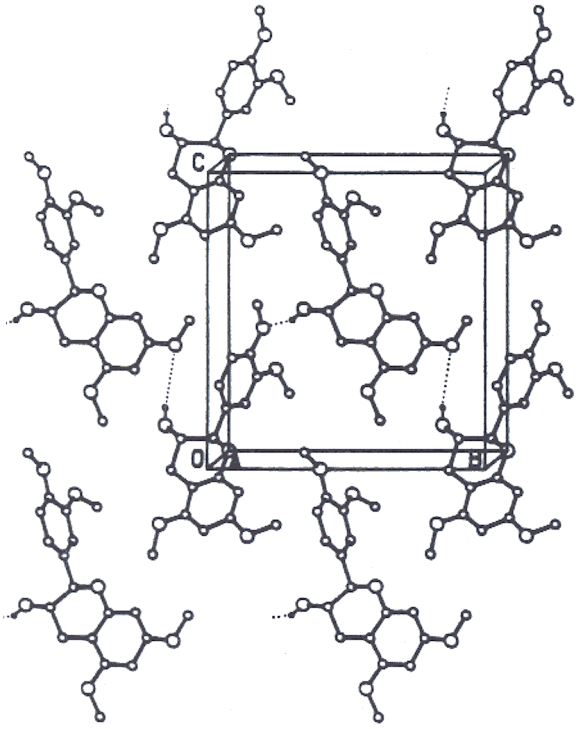

Figure 3. Illustration of the pattern of the intermolecular hydrogen bonds.

heterocyclic ring, C(2) and C(3) are the furthest out of the mean plane. Atom C(2) is above the mean plane by 42.7 and 30.0 pm for crystal structure A and B, respectively. Atom C(3) is 41.2 and 49.2 pm below the mean plane for A and B, respectively. The aromatic ring attached to C(2) and the hydroxy group attached to C(3) are in equatorial positions for both crystal structures.

The fused ring system of tetra-*O*-methyl-(+)-catechin can be compared with the systems in (−)-epicatechin[10] and in two derivatives of (+)-catechin. The two derivatives chosen for this purpose are 8-bromotetra-*O*-methyl-(+)-catechin, which is the first crystal structure reported for molecules related to catechin or epicatechin,[11] and penta-*O*-acetyl-(+)-catechin, which is the derivative that has an axial substituent at C(2) and is conformationally disordered in the crystal.[14] Similar to the heterocyclic ring in tetra-*O*-methyl-(+)-catechin, C(2) lies above and C(3) lies below the mean plane in 8-bromotetra-*O*-methyl-(+)-catechin and (−)-epicatechin. The positions of these two atoms are reversed with respect to the mean plane in penta-*O*-acetyl-(+)-catechin, for which the conformation of the heterocyclic ring places the diacetoxyphenyl substituent at C(2) in an axial position. In all of the other structures, the substituent at C(2) occupies an equatorial position. The substituent at C(3) is in an equatorial position in tetra-*O*-methyl-(+)-catechin and in 8-bromotetra-*O*-methyl-(+)-catechin. The closest correspondence between the structures of the heterocyclic rings in tetra-*O*-methyl-(+)-catechin and the other three structures is between structure B and (−)-epicatechin. In this pair C(2) is above the plane by 30.0 or 26.3 pm, and C(3) is below the plane by 49.2 or 49.5 pm. Therefore structure B has a heterocyclic ring conformation for which there is precedence in another crystal structure.

The theoretical analysis, using MM2,[18] of the conformations of 16 dimers of (+)-catechin and/or (−)-epicatechin reveals a family of structures for the heterocyclic ring that can be described as being close to the line

$$d_2 = 76 + d_3 \qquad (1)$$

where d_i is the distance (in pm) of C(i) from the mean plane of the heterocyclic ring.[3] Both structure A and structure B have heterocyclic rings with conformations that are close to the prediction from Eq. (1). The theoretical analysis with MM2 finds a conformation for the bottom unit in (+)-catechin-(4β → 8)-(+)-catechin that is very close to the one observed for structure A of tetra-*O*-methyl-(+)-catechin. This conformation has C(2) 40 pm above the plane, and C(3) 38 pm below the plane. Thus there is excellent experimental precedence for the heterocyclic ring conformation in structure B, and precedence from MM2 calculations for the heterocyclic ring conformation in structure A and in structure B.

Conformational Energies

The two crystal structures were optimized using the force field found in Sybyl version 5.32. The dihedral angle for rotation about the C(3)—O(2) bond

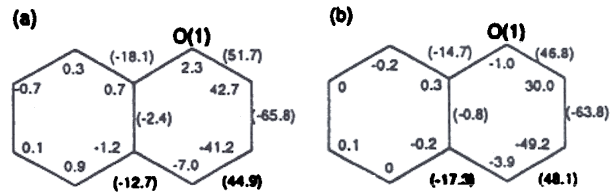

Figure 4. Distances (pm) out of the mean plane of the aromatic ring for carbon and oxygen atoms in the fused ring system of crystalline (a) tetra-*O*-methyl-(+)-catechin crystal A and (b) tetra-*O*-methyl-(+)-catechin crystal B. Numbers in parentheses are the dihedral angles (°).

moves from −83° to −63° upon optimization of structure A, but in the optimization of structure B this dihedral angle stays at about 180°. The dihedral angle at the C(3) — O(2) bond was monitored in a 4.5-ns molecular dynamics trajectory computed for an isolated molecule of tetra-*O*-methyl-(+)-catechin at 300 K. The simulation reveals three rotational states at the C(3) — O(2) bond, ±60° and 180°. The average time the molecule remains in one of these states is approximately 0.2 ns.

After optimization the dihedral angles for the O(6) — C(20) bond are 60°, independent of the starting structure. The values in the crystalline state are 47° and 65° for structure A and structure B, respectively. In the molecular dynamics simulation, the three rotational states observed for the O(6) — C(20) bonds are ±60° and 180°. The magnitude of the fluctuations about each state in the simulations is about ±25°. Thus the two conformations seen in the crystalline state will interconvert very rapidly in an environment in which the molecule is dynamically active.

The dihedral angle at C(2) — C(11) experiences a large rotation upon optimization. In the optimized structures its values are 136.0° and 138.5°. The response of the dihedral angle at C(2) — C(11) is coupled with the conformation of the heterocyclic ring. The distinct heterocyclic ring conformations in structure A and structure B converge to a single conformation upon optimization. The results, expressed in terms of dihedral angles for the six bonds in the heterocyclic ring, are summarized in Figure 5. The average change in dihedral angle is of magnitude 3°, and the largest change is 6°. In the optimized structures, C(2) is above the mean plane by 42–43 pm, and C(3) is below the mean plane by 35–36 pm. The dimethoxyphenyl substituent at C(2) and the hydroxy group at C(3) are in equatorial positions. The optimized structure is close to the original structure A and structure B, and has positions of C(2) and C(3) that are consistent with Eq. (1).

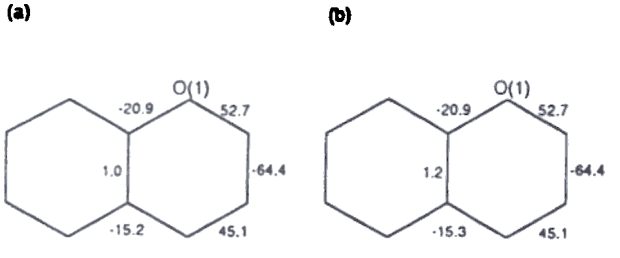

Figure 5. Dihedral angles after optimization of a single molecule in vacuo, starting from structure A (panel a) or structure B (panel b).

Proton NMR Coupling Constants and the Equatorial ⇌ Axial Interconversion of the Heterocyclic Ring

In the crystal, the heterocyclic ring adopts a conformation that places the dimethyoxyphenyl substituent at C(2) in an equatorial position. In this structure, the dihedral angle defined by H(2) — C(2) — C(3) — H(3) is 178°. In solution, the coupling constant for H(2) — H(3), $^3J_{2,3}$, is 8.1 Hz. Using the dihedral angle found in the crystal, Altona and co-workers' generalized Karplus equation can be used to calculate coupling constants:[15,19]

$$^3J_{H,H} = 13.22\cos^2\phi - 0.99\cos\phi + \sum \Delta\chi_i[0.87 - 2.46\cos^2(\xi_i\phi + 19.9|\Delta\chi_i|) \quad (2)$$

In this equation, ϕ is the proton–proton dihedral angle, $\Delta\chi_i = \chi_i - \chi_H$, where χ is the Huggins[20] electronegativity of hydrogen, H, and the substituent i, and ξ is either +1 or −1 depending on the orientation of the substituent as defined by Altona and coworkers.[19] The calculated coupling constant for the equatorial conformation, which is observed in the crystal, is 10.0 Hz. For the axial conformation, which has a dihedral angle defined by H(2) — C(2) — C(3) — H(3) of −60° (+300°), the calculated coupling constant is 3.0 Hz. Porter and co-workers[15] previously concluded that the heterocyclic ring conformations in solution for catechin, epicatechin, and their *O*-substituted derivatives were equilibrium mixtures of both axial and equatorial conformations, which would explain the value of the experimental coupling constant between the coupling constants calculated for the axial and equatorial conformations.

To investigate the heterocyclic ring conformations giving rise to the experimental coupling constant, a 4.5-ns molecular dynamics trajectory was computed using Sybyl 4.1c at 300 K in vacuo. Figure 6 depicts the dihedral angle for rotation about the C(2) — C(3) bond as a function of time. It shows that the heterocyclic ring converts between the equatorial ($\phi \sim 180°$) and axial ($\phi \sim 300°$) conformations throughout the trajectory. This transition between the two states explains the experimentally observed coupling constant having a value between the values calculated for the equatorial and axial conformations. This conclusion agrees with Porter and co-workers' results.[15] In addition, Hoch, Dobson, and Karplus observed that poor agreement between the coupling constants calculated from the crystal structure and the experimental coupling constant indicates that more than one conformation exists for the dihedral angle.[21] The time scale for

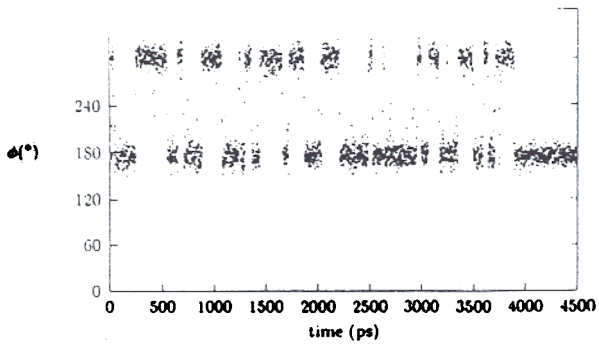

Figure 6. Trajectory for the dihedral angle at C(2)-C(3) bond, which defines axial and equatorial conformations.

the transition between the two states observed in the molecular dynamics simulation is very fast in comparison to the time scale of ^{1}H-nmr.

Figure 7 shows the probability $P(\phi)$ of occurrence of a given dihedral angle for rotation about the C(2) — C(3) bond. As observed in Figure 6, two states are seen with similar distributions about their average dihedral angles. However, the equatorial conformation is populated to a greater extent.

In addition to the dihedral angle for rotation about the C(2) — C(3) bond, the dihedral angle for rotation about the C(2) — C(11) bond was monitored in order to understand the equatorial ⇌ axial interconversion. This dihedral angle is defined by atoms O(1) — C(2) — C(11) — C(12). Figures 8a and 8b show the probability $P(\phi)$ of occurrence of a given dihedral angle for rotation about the C(2) — C(11) bond when the heterocyclic ring is in the axial conformation and equatorial conformation, respectively. For both axial and equatorial conformations, two states approximately 180° apart exist for rotation about the C(2) — C(11) bond. For the axial conformation, the two states are centered at approximately 0° and 180°. These two states occur at approximately 140° and 320° for the equatorial conformation. No correlation was found between the equatorial ⇌ axial interconversion of the heterocyclic ring and the transitions between the states for the rotation about the C(2) — C(11) bond.

A predicted coupling constant can be calculated from the molecular dynamics trajectory as

$$J = p_{ax}J_{ax} + p_{eq}J_{eq} \tag{3}$$

$$p_i = \frac{t_i}{\sum t_i} \tag{4}$$

with t_i being the total time spent in either the axial or the equatorial conformation during the entire trajectory. J_{ax} and J_{eq} are the coupling constants calculated for $\langle\phi\rangle_{ax}$ and $\langle\phi\rangle_{eq}$, respectively, that are obtained from the molecular dynamics trajectory. In Table II, p_{ax} and p_{eq} are given for different lengths of the trajectory. As shown, the probabilities for the conformations reach constant values after 3 ns,

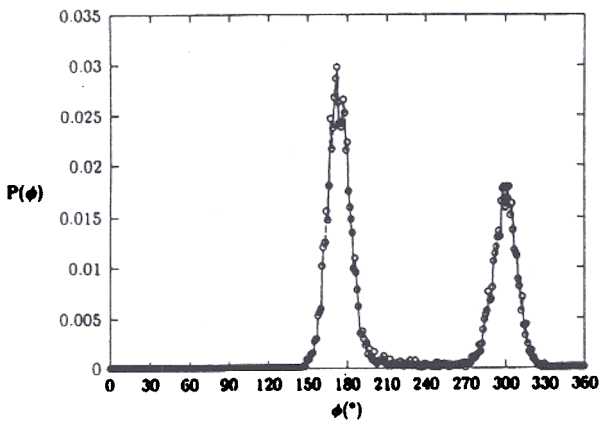

Figure 7. Average populations for the dihedral angle at C(2)-C(3).

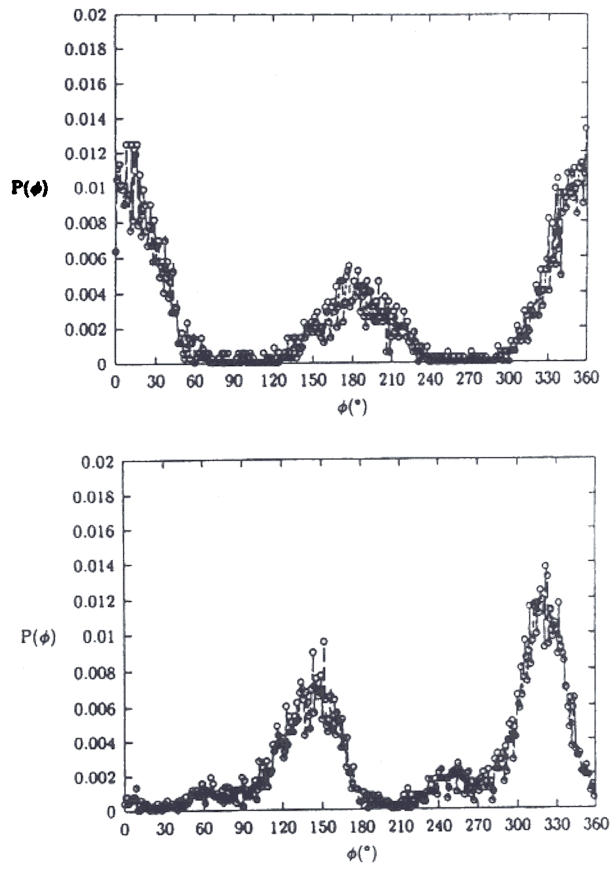

Figure 8. Average populations for the dihedral angle at C(2)-C(11) when the heterocyclic ring is in axial conformation (a) or equatorial conformation (b).

Table II Probabilities of Axial and Equatorial Conformations

Trajectory Length (ns)	$p_{eq} = 1 - p_{ax}$
1.0	0.5
2.0	0.5
3.0	0.6
4.0	0.6
4.5	0.6

which are 0.4 and 0.6 for p_{ax} and p_{eq}, respectively. The average value of the dihedral angle is 300.1° for the axial conformation and 174.4° for the equatorial conformation. Using these dihedral angles in Eq. (2), J_{ax} is 3.1 Hz and J_{eq} is 10.0 Hz. The predicted coupling constant that is calculated using Eq. (3) is 7.3 Hz. This predicted coupling constant is in reasonable agreement with the experimental result of 8.1 Hz.

As verification of the calculated probabilities, a second molecular dynamics trajectory was computed for 4.5 ns at 300 K. In this trajectory, the molecule was in a different conformation at the point of initiation. Similar results were observed for the dihedral angle for rotation about the C(2) — C(3) bond as a function of time. The values of p_{ax} and p_{eq} were 0.4 and 0.6, respectively, which agree with the probabilities calculated from the first trajectory.

CONCLUSION

Tetra-*O*-methyl-(+)-catechin exists in two different conformations in the unit cell. The dimethoxyphenyl substituent at C(2) and the hydroxy group at C(3) are in the equatorial position in both of these conformations. The conformations observed in the crystalline state exist because of intermolecular hydrogen bonding. In solution, however, the axial and equatorial conformations of the heterocyclic ring are present in approximately 40/60 relative populations. The interconversion of the axial and equatorial conformations is fast on the ^{1}H-nmr time scale, but accessible on the molecular dynamics time scale.

This research was supported by the U.S. Department of Agriculture, 87-FSTY-9-0256 and 91-02034. A full description (coordinates, thermal parameters, bond lengths, bond angles, torsion angles, hydrogen-bond geometry, anisotropic thermal parameters, and structure factor amplitudes) of the crystal structure is contained in 47 pages of supplementary material, which is available from FRF or WLM.

REFERENCES

1. Haslam, E. (1977) *Phytochemistry* **16**, 1625–1640.
2. Hemingway, R. W. & Karchesy, J. J., Eds. (1989) *Chemistry and Significance of Condensed Tannins*, Plenum, New York.
3. Viswanadhan, V. N. & Mattice, W. L. (1986) *J. Comput. Chem.* **7**, 711–717.
4. Viswanadhan, V. N. & Mattice, W. L. (1987) *J. Chem. Soc. Perkin Trans. 2*, 739–743.
5. Cho, D., Mattice, W. L. & Porter, L. J. (1990) *Biopolymers* **29**, 57–60.
6. Bergmann, W. R., Barkley, M. D., Hemingway, R. W. & Mattice, W. L. (1987) *J. Am. Chem. Soc.* **109**, 6614–6619.
7. Cho, D., Tian, R., Porter, L. J., Hemingway, R. W. & Mattice, W. L. (1990) *J. Am. Chem. Soc.* **112**, 4273–4277.
8. Viswanadhan, V. N., Bergmann, W. R. & Mattice, W. L. (1987) *Macromolecules* **20**, 1539–1543.
9. Bergmann, W. R., Viswanadhan, V. N. & Mattice, W. L. (1988) *J. Chem. Soc. Perkin Trans. 2*, 45–47.
10. Fronczek, F. R., Gannuch, G., Mattice, W. L., Tobiason, F. L., Broeker, J. L. & Hemingway, R. W. (1984) *J. Chem. Soc. Perkin Trans. 2*, 1611–1616.
11. Engel, D. W., Hattingh, M., Hundt, H. K. L. & Roux, D. G. (1978) *J. Chem. Soc. Chem. Commun.* 695–696.
12. Einstein, F. W. B., Kiehlmann, E. & Wolowidnyk, E. K. (1985) *Can. J. Chem.* **63**, 2176–2180.
13. Porter, L. J., Wong, R. Y. & Chan, B. G. (1985) *J. Chem. Soc. Perkin Trans. 1*, 1413–1418.
14. Fronczek, F. R., Gannuch, G., Mattice, W. L., Hemingway, R. W., Chiari, G., Tobiason, F. L., Houglum, K. & Shanafelt, A. (1985) *J. Chem. Soc. Perkin Trans.* **2**, 1383–1386.
15. Porter, L. J., Wong, R. Y., Benson, M., Chang, B. G., Viswanadhan, V. N., Gandour, R. D. & Mattice, W. L. (1986) *J. Chem. Res.* S86–S87, M830.
16. Weinges, K., Bahr, W., Ebert, W., Goritz, K. & Marx, H.-D. (1969) in *Fortschritl der Chemic Organisher Naturstoffe*, Zechmeister, L., Ed., Springer-Verlag, New York.
17. Sheldrick, G. M. in Sheldrick, G. M., Krüger, C. & Goddard, R., Eds. (1985) *Crystallographic Computing 3*, Oxford University Press, New York, pp. 175–189.
18. Allinger, N. L. & Yuh, Y. H. (1980) *Quantum Chem. Program Exchange* **12**, 395.
19. Haasnoot, C. A. G., deLeeuw, F. A. A. M. & Altona, C. (1980) *Tetrahedron* **36**, 2783–2792.
20. Huggins, M. L. (1953) *J. Am. Chem. Soc.* **75**, 4123–4126.
21. Hoch, J. C., Dobson, C. M. & Karplus, M. (1985) *Biochemistry* **24**, 3831–3841.

Received March 27, 1992
Accepted July 22, 1992